

Original Article

Pyrrolidine Dithiocarbamate Attenuates Cardiocyte Apoptosis and Ameliorates Heart Failure Following Coronary Microembolization in Rats

Li et al. PDTC Improves Heart Failure

Shumei Li, Jun Fang, Lianglong Chen

Department of Cardiology, Union Hospital, Fujian Medical University, 29 Xin-Quan Road, Fujian, China

Address for Correspondence: Jun Fang, Department of Cardiology, Union Hospital, Fujian Medical University, 29 Xin-Quan Road, Fujian, China

Phone: +86 13358202350 e-mail: ptfangjun@126.com - 13763859969@163.com

Received: 6 March 2019

Accepted: 28 May 2019

DOI: 10.4274/balkanmedj.galenos.2019.2019.3.8

Cite this article as:

Li S, Fang J, Chen L. Pyrrolidine Dithiocarbamate Attenuates Cardiocyte Apoptosis and Ameliorates Heart Failure Following Coronary Microembolization in Rats. *Balkan Med J*

Background: To evaluate the effects of specific NF- κ B inhibitor pyrrolidine dithiocarbamate (PDTC) on cardiocyte apoptosis and cardiac function in a rat model of heart failure (HF).

Study Design:

Methods: A stable and reproducible rat HF model (n=64) was established by injecting homologous microthrombotic particles (MTPs) into the left ventricle and obstructing the ascending aorta to produce coronary microembolization. HF rats were randomized into untreated (HFu) and PDTC-treated (HFp) groups, the latter intraperitoneally receiving an injection of PDTC (100 mg/kg/day) 1 h before the operation and on postoperative Days 1 to 7. Thirty-two Sprague–Dawley rats served as the sham group; Eight rats from each group were sacrificed on days 1, 3, 7, 14 post-operatively. Masson's trichrome staining was used to determine the micro-fibrotic area, indicating the severity of myocardial loss (SML); the terminal transferase UTP nick end labeling (TUNEL) staining to detect apoptotic cardiomyocytes. Echocardiography and hemodynamics were performed to evaluate the left ventricular (LV) function.

Results: HF rats exhibited pathological changes evidenced by patchy myocardial fibrosis, remarkably-increased SML, and persistently-reduced LV function. At the termination of observation, compared with those of the HFu group, PDTC administration significantly reduced myocardial infarctlet size by 28% ($p=0.001$) and suppressed cardiocyte apoptosis ($7.17\pm 1.47\%$ vs. $2.83\pm 0.75\%$, $p<0.001$); cardiac function parameters of the HFp group, such as LVEF ($80\pm 4\%$ vs. $61\pm 6\%$), LV +dP/dt max (4828 ± 289 vs. 2918 ± 276 mmHg s⁻¹), LV -dP/dt max (4398 ± 269 vs. 2481 ± 365 mmHg s⁻¹) and

LVSP (126±13 vs. 100±10 mmHg), were significantly increased and LVEDP reduced (18±2 vs. 13±1 mmHg) ($p<0.001$, for all).

Conclusion: The rat model can properly mimic heart failure via coronary vessel embolization. PDTC treatment can reduce cardiocyte apoptosis and improve myocardial infarction which may benefit patients with HF secondary to myocardial infarction.

Keywords: NF- κ B, pyrrolidine dithiocarbamate, cardiocyte apoptosis, cardiac function

Congestive heart failure (HF) is a serious and complex clinical syndrome with high morbidity, disability rate and mortality. Patients who are afflicted with coronary heart disease, especially those receiving percutaneous coronary intervention (PCI) can easily become prone to HF due to coronary microembolization [1]. The current study, therefore, created a reproducible and stable rat model of chronic heart failure using homologous blood emboli to produce coronary microembolization. This paper outlines the technique and characterizes its hemodynamic effects in the rats.

In cardiovascular disorders, the available literature has documented that nuclear factor- κ B (NF- κ B) is highly activated [2, 3, 4]. It can enhance the inflammatory response in unstable angina pectoris (UA) patients whose C-reactive protein (CRP) level was increased [3] and can be selectively and markedly activated in peripheral blood leukocytes of people with UA before malignant cardiac events, which may be mechanistically engaged in the plaque disruption that can induce acute coronary artery syndromes [5]. Recent studies report that NF- κ B mediates autophagy induction to aggravate myocardial injury in cardiac ischemia/reperfusion injury (I/R) and post-MI cardiac remodeling [6] and is associated with cardiac hypertrophy and hypertension by regulating cytokines and oxidative stress [7]. More evidence shows that NF- κ B regulates consequent inflammatory cascade and apoptosis-associated genes, which is a confirmed cause for progressive contractile dysfunction and cardiac injury [8]. A previous study of NF- κ B-null mice reports ameliorated cardiac function after myocardial infarction [9]. In addition, oxidative stress can activate NF- κ B and trigger the transcription of pro-apoptotic genes, such as Fas, Bax, and FasL, resulting in myocardial cell apoptosis and heart failure. A study has documented that pyrrolidine dithiocarbamate (PDTC), an antioxidant, specifically suppresses NF- κ B activation [10]. However, few articles have targeted at the role of NF- κ B inhibitor in heart failure. Therefore, the present study attempted to investigate whether PDTC-induced inhibition of NF- κ B would reduce cardiac injury and improve progression of contractile dysfunction in HF rats.

Methods

Animal preparation and experimental procedures

Sprague Dawley (SD) rats (weighed 280–320 grams) were provided from the animal center of Medical University. These animals were raised in conditions with controlled humidity, lighting cycle, and temperature, and allowed access to water and rat chow ad libitum. The study protocol observed *The Guide for the Care and Use of Laboratory Animals* (NIH Publication NO. 85-23, revised 1996) and received approval from the Clinical and Animal Research Ethics Committee of Medical University.

Preparation of homologous microthrombotic particles

Male SD rats were sedated through an intraperitoneal injection of ketamine (75 mg/kg) and diazepam (7.5 mg/kg) 36 hours before the experiment. Prior to each injection, 7 milligrams of the particles ($\sim 15\text{--}19 \times 10^9$) were thoroughly suspended in calcium-free Dulbecco's phosphate-buffered saline (PBS) with a vortex agitator. The tail blood (500ul per rat) was obtained and stored at room temperature to allow clot formation. The latter was fragmented with a homogenizer and filtered with a 38 μ m screen to obtain microthrombi (microthrombo-emboli), which were between 10-30 μ m as measured by a

micrometer.

Creation of HF model

After 36 hours, the rats were reanesthetized with ether and were ventilated with a small animal ventilator. Next, a thoracotomy along the midline was conducted with the mammalian arteries ligated. Afterwards, a sternotomy was performed between the second and third intercostal spaces. The pericardium was next cut open, exposing the ascending aorta. A bolus of the microembolic suspension in PBS was injected into the left ventricular (LV) chamber with a 26-gauge needle while the ascending aorta was occluded for 10 s. Sutures were used to close the thoracic cavity and skin incision. The age-matched sham group received the same surgical procedure and a PBS injection of the same volume.

Experimental protocol

A total of 32 SD rats received a sham operation and 64 rats the surgery previously described to establish an HF model, which was randomized into an untreated HF group (HFu, n = 32) or PDTC-treated HF group (HFp, n = 32). The HF rats were sacrificed at postoperative days 1, 3, 7, 14, forming 4 subgroups (n = 8, each). PDTC (Sigma, USA) in a 0.9% NaCl solution was intraperitoneally administered at a dosage of 100 mg/kg/day, which started one hour before the operation and continued for 7 postoperative days. The PDTC doses have been proved to effectively blunt NF-KB activation with no significant toxicity [11].

Study protocols

Echocardiographic study

The rats were sedated for the echocardiography procedure, as previously described. Echocardiography with two-dimensional and M-mode imaging modalities was conducted with a medical diagnostic system (VIVID-7, GE Medical System, USA) equipped with a 10 MHz phased-array transducer. Electrocardiographic measurements were recorded simultaneously with respiratory tracings. The LV end-diastolic diameter (LVEDD; at the R wave of the ECG) and the end-systolic diameter (LVESD; at the peak inward motion of the endocardial excursion) were recorded using the M-mode tracings of the level of the chordae tendineae at the end of expiration in the LV short axis view. A cubic formula was employed to calculate the LV ejection fraction (LVEF). For all parameters, at least three consecutive cardiac cycles were averaged. The echocardiographic readings were recorded and stored throughout the experiment.

Hemodynamic study

Hemodynamic measurements were performed under general sedation and a 20-gauge polyethylene cannula was inserted from the right carotid artery into the left ventricle. The maximum change of LV pressure during isovolumic contraction (LV+dP/dt max) and relaxation (LV -dP/dt max) was calculated from the LV pressure traced with a resistance-capacitance (RC) analog differentiator and the LV systolic pressure. The hemodynamic and functional parameters were recorded in each procedure.

Histopathological study

After the harvest, the hearts were fixed in 10% formalin, embedded and cut into slices (5 μ m thick). Trans-sections from the chordae tendineae, papillary muscle, mitral valve, and near-apex of the LV were subject to morphological assessment.

Hematoxylin and eosin staining was performed on the sections to evaluate the general morphology. Masson's trichrome staining showed micro-fibrotic foci at the chronic phases (14 post-operative days), indicating myocardial loss. The area taken by fibrotic foci, representing the severity of myocardial loss, was calculated with the following equation: severity of myocardial loss (SML; %) = total fibrotic

area/total area of a whole section x 100. The whole section was morphologically quantified using an image processing system (Image-Pro Plus 5.0 Media Cybernetics, Inc, USA).

Detection of apoptosis by TUNEL assay

Myocardial tissues were placed in a paraffin block and transversely cut into sections (5- μ m) according to the instructions of an in situ cell death detection kit (Roche, Switzerland). The apoptosis of cardiomyocytes was indicated by the terminal transferase UTP nick end labelling (TUNEL) staining. The treated myocardial tissue was heated in a sodium citrate solution and dissolved with proteinase K for DNA exposure. The resulted DNA strand breaks were labelled with a terminal transferase enzyme, with dUTP molecules conjugated to horseradish peroxidase, and visualized by immunohistochemistry. TUNEL-positive nuclei of cardiomyocytes (brownish red) were regarded as apoptotic cells from 10 random fields (\approx 400) per section with a total of 100 nuclei per field. The severity of apoptosis was evaluated by the apoptosis index (AI), calculated by the number of TUNEL-positive nuclei over the total nuclei.

Statistical analysis

SPSS 13.0 for Windows was used to analyze the data (mean \pm SD). Intergroup comparisons were performed by the one-way ANOVA followed by Dunnett's modified test. Statistical significance was set at $p < 0.05$.

Results

General conditions of experimental rats

All the animals in the sham group survived the operation. Six rats in the HFu group died within 1 week after coronary microembolization and the survivors showed various degrees of mental exhaustion, dyspnea, decreased activity and eating, and shock in severe cases. Autopsy of dead rats showed bilateral pulmonary congestion and pleural effusion, suggesting sudden cardiac death and possible death from heart failure. Two rats died in the HFp group.

Pathohistological findings

After Masson's trichrome staining, qualitative analysis revealed multiple patchy fibrosis in the HF group on post-operative day 14. A heterogeneous distribution characterized the transmural changes, more involvement in the subendocardial, instead of the subepicardial, region (Fig. 1). Compared with the sham group, SML was significantly increased in CME, (21.25 \pm 3.54% vs. 0.66 \pm 0.35%; $p < 0.001$) (Table 1). PDTC administration significantly reduced the myocardial infarctlet size in the HFp group. On post-operative day 14, SML markedly decreased in the HFp group when in comparison with the HFu group (by 28%, $p = 0.001$).

Effects of PDTC on cardiocyte apoptosis

The death of cardiac muscle cells occurs in two forms: necrosis and apoptosis. The comparison with the sham group revealed that the apoptosis increased in the myocardial microinfarct zone of the HF group (Figure 2). On postoperative day 1, 3, 7, 14, cardiocyte apoptosis indices were 13.33 \pm 2.16%, 19.67 \pm 2.58%, 11.50 \pm 2.74%, and 7.17 \pm 1.47% ($p < 0.001$, for all). PDTC treatment significantly reduced myocardial apoptosis rate (Table 2).

Alterations of cardiac function

Compared with the sham counterparts, the HFu rats reported markedly lower LVSP, LV +dP/dt max, LV -dP/dt max, and LVEF at all corresponding stages (Table 3). After coronary microembolization, on day 14, relative to the measurements in the sham group, LVEF (61 \pm 6% vs. 90 \pm 4%, $p < 0.01$), LVSP (100 \pm 10 vs. 135 \pm 10 mmHg), LV +dP/dt max (2918 \pm 276 vs. 5707 \pm 544 mmHg s⁻¹), and LV -dP/dt max (2481 \pm 365 vs. 4974 \pm 767 mmHg s⁻¹) significantly decreased while LVEDP increased (3 \pm 1 vs.

18±2mmHg) ($p<0.001$, for all). At the termination of observation, in the HFp group, LVEF (80±4% vs. 61±6%), LV +dP/ dt max (4,828±289 vs. 2918±276 mmHg s-1), LV -dP/ dt max (4,398±269 vs. 2481±365 mmHg s-1), and LVSP (126±13 vs. 100±10 mmHg) were significantly increased while LVEDP was markedly reduced (18±2 vs. 13±1 mmHg) ($p<0.001$, for all).

These data indicate that at the acute phase, LV diastolic and systolic functions are obviously impaired in the untreated HF rats, and deteriorate continuously to subacute and the chronic phases; and that LV functions in PDTC-treated rats are significantly improved at all phases.

Discussion

The syndrome of HF is associated with multiple adaptations and pathophysiological alterations. These include upgraded systemic vascular resistance, marked LV dysfunction, dilatation, and activated neuroendocrine system. An understanding of the changes that take place during HF is critical to the study of the disease history and to the efficacy and timing of the interventions that are necessary for reversing the process, or at least retard its progression, and the history of the disease. Developing an animal model that accurately portrays HF can be of use in heart failure studies.

Coronary microembolization plays a role in many disorders, including acute coronary syndrome with ST elevation and non-ST elevation, sudden cardiac death. It often occurs after thrombolytic therapy or during coronary interventions [12-15]. It can also affect myocardial perfusion, featured by low or no-reflow, which can result in myocardial infarction and infarctlet production, coronary reserve reduction, arrhythmias, and contractile dysfunction [16-18]. Studies have documented that serious coronary microembolization can induce chronic heart failure [19,20].

The established models are evaluated by cardiac function examinations which include cardiac catheterization and ultrasonic cardiogram. According to this model, rats with LVEDP >15 mmHg are thought to have severe CHF [21]. The myocardial infarction area is correlated well with cardiac function, and when the infarction area surpasses 20%, obvious contractile dysfunction or cardiac shock is induced. Our model illuminated many sequelae of HF, such as severely impaired LV diastolic and systolic functions, reduced cardiac function and LV dilation. The findings indicate that chronic heart failure by a loss of contractile myocardium can be successfully created by using homologous microthrombotic particles. This study's rat HF approach differs from previous trials: previous studies use a single or multiple intracoronary injection of microspheres to induce myocardial dysfunction and the operative procedure is relatively easy [22]. However, in the current study, the experimental micro-emboli obtained are abundant in fibrin, platelets, and other particles, which is an attractive feature of the HF model. This model closely mimics the aspects of clinical coronary emboli and can be used to simulate clinical CME conditions. The overall area of the infarctlet is generally unchanged and can be controlled, for a preliminary experiment indicates that it was dose-dependent, although the microinfarcts were unpredictably distributed.

As a transcription factor sensitive to redox, NF- κ B exists in cell types that have p50/65 heterodimer. In general, inactive NF- κ B dimers are bound to the inhibitor of NF- κ B proteins (I κ Bs) but still in the cytosol. Stimuli such as reactive oxygen species (ROS) may activate NF- κ B. The activated latter may then be translocated into the nucleus, where the specific target genes regulating inflammation and apoptosis are in turn activated. Thus, NF- κ B is a major initiator in ROS mediated cardiocyte apoptosis and excessive cardiac fibrosis [23]. Accumulating evidence suggests that PDTC, as a powerful antioxidant and inhibitor of NF- κ B, can be a candidate therapeutic means for many cardiac diseases [24]. PDTC protects against adriamycin-induced myocardial apoptosis, reduces I/R-associated myocardial no-reflow and so on [25,26]. So, using this heart failure model, we further studied the

effects of PDTC on cardiocyte apoptosis and cardiac pathophysiology of heart failure. The results of the present study are consistent with the evidence that myocyte apoptosis aggravates in the untreated infarcted hearts [27,28]. The current study further reveals that PDTC treatment can markedly ameliorate myocyte apoptosis in a worsening heart failure.

In cardiac pathology, the role of cardiac myocyte apoptosis are still speculative. However, it is intriguing that a progressive loss of cardiac myocytes can in part be compensated by fibroblast cell proliferation, which further deteriorates cardiac function. Furthermore, the degree of cardiomyocyte apoptosis is intriguingly associated with the severity of left ventricular dilation and systolic dysfunction in acromegaly-associated cardiomyopathy in man [29]. Other reports show that the shift from concentric left ventricular hypertrophy to the dysfunction of LV dilatation and systolic pressure is linked with aggravated myocyte apoptosis [30, 31]. Thereby, the antioxidant therapy-attenuated programmed cell death may possess a beneficial therapeutic value for treating congestive heart failure. This study also attempts to probe into the hemodynamic effects of the antioxidant therapy, for research has evidenced that oxidative stress has adverse effects on myocardial function [32,33]. Attenuated oxidative stress within the myocardium probably suppresses the deteriorated myocardial contractility. In our HF model, antioxidant treatment obviously attenuated the cardiac dysfunction. In this context, we speculate that the apparent benefits of PDTC treatment in heart failure may be partly due to its antioxidant effect and partly to the PDTC-induced inhibited transcription of several pro-apoptotic genes, thus leading to apoptosis inhibition and cardiac function improvement. Treatment with antioxidant PDTC may have a promising value in treating congestive heart failure, but further investigation is needed.

Financial: The study was supported by the funds for the innovation of science and technology, fujian province (grant no.2017Y9007).

REFERENCES

1. Heusch GJ, Kleinbongard P, Böse D, et al. Coronary microembolization: from bedside to bench and back to bedside. *Circulation* 2009; 120:1822-1836.
2. Adhikari N, Charles N, Lehmann U, et al. Transcription factor and kinase-mediated signaling in atherosclerosis and vascular injury. *Curr Atheroscler Rep* 2006; 8:252-260.
3. Liuzzo G, Santamaria M, Biasucci LM, et al. Persistent activation of nuclear factor kappa-B signaling pathway in patients with unstable angina and elevated levels of C-reactive protein evidence for a direct proinflammatory effect of azide and lipopolysaccharide-free C-reactive protein on human monocyte via nuclear factor kappa-B activation. *J Am Coll Cardiol* 2007; 49:195-197.
4. Pierce GL, Lesniewski LA, Lawson BR, et al. Nuclear factor- κ B activation contributes to vascular endothelial dysfunction via oxidative stress in overweight/obese middle-aged and older humans. *Circulation* 2009; 119: 1284-1292.
5. Michael E, Ritchie. Nuclear Factor- κ B is selectively and markedly activated in humans with unstable angina pectoris. *Circulation* 1998; 98: 1707-1713.
6. Zeng M, Wei X, Wu Z, et al. NF- κ B-mediated induction of autophagy in cardiac ischemia/reperfusion injury. *Biochem Biophys Res Commun* 2013; 436:180-185.
7. Yu XJ, Zhang DM, Jia LL, et al. Inhibition of NF- κ B activity in the hypothalamic paraventricular nucleus attenuates hypertension and cardiac hypertrophy by modulating cytokines and attenuating oxidative stress. *Toxicol Appl Pharmacol* 2015; 284: 315-322.
8. Gordon JW, Shaw JA and Kirshenbaum LA. Multiple facets of NF- κ B in the heart: to be or not to

NF- κ B. *Circ Res* 2011; 108: 1122-1132.

9. Frantz S, Hu K, Bayer B, et al. Absence of NF-kappaB subunit p50 improves heart failure after myocardial infarction. *FASEB* 2006; 20:1918-1920.
10. Scherck R, Meier B, Mannel DN, et al. Dithiocarbamates as potent inhibitors of nuclear factor kB activation in intact cells. *J Exp Med* 1992; 175:1181-1194.
11. Liu SF, Ye X, Malik AB. Inhibition of NF-kB activation by pyrrolidine dithiocarbamate prevents in vivo expression of proinflammatory genes. *Circulation* 1999; 100:1330-1337.
12. Böse D, von Birgelen C, Zhou XY, et al. Impact of atherosclerotic plaque composition on coronary microembolization during percutaneous coronary interventions. *Basic Res Cardiol* 2008; 103:587-597.
13. Herrmann J. Peri-procedural myocardial injury: 2005 update. *Eur Heart J* 2005; 26: 2493-2519
14. Kawano H, Hayashida T, Ohtani H, et al. Histopathological findings of the no-reflow phenomenon following coronary intervention for acute coronary syndrome. *Int Heart J* 2005; 46: 327-332.
15. De Maria GL, Patel N, Kassimis G, et al. Spontaneous and procedural plaque embolisation in native coronary arteries: pathophysiology, diagnosis, and prevention. *Scientifica (Cairo)* 2013; 2013: 364247-364262.
16. Skyschally A, Schulz R, Haude M, et al. Coronary microembolization, perfusion-contraction mismatch secondary to myocardial inflammation. *Herz* 2004; 29: 777-781.
17. Jianying Ma, Juying Qian, Junbo Ge, et al. Changes in left ventricular ejection fraction and coronary flow reserve after coronary microembolization. *Arch Med Sci* 2012; 8: 63-69.
18. Gerd Heusch, Peter Libby, Bernard Gersh, et al. *Lancet Seminar: Cardiovascular Remodelling in Coronary Artery Disease and Heart Failure.* *Lancet* 2014; 383: 1933-1943.
19. Reuben M. Thomas, Sang Yup Lim, Beiping Qiang, et al. Distal coronary embolization following acute myocardial infarction increases early infarct size and late left ventricular wall thinning in a porcine model. *J Cardiovasc Magn Reson* 2015; 17: 106-119.
20. Gill RM, Jones BD, Corbly AK, et al. Cardiac diastolic dysfunction in conscious dogs with heart failure induced by chronic coronary microembolization. *Am J Physiol Heart Circ Physiol* 2006; 291: H3154-H3158.
21. Nielsen S, Terris J, Andersen D, et al. Congestive heart failure in rats is associated with increased expression and targeting of aquaporin-2 water channel in collecting duct. *Proc Natl Acad Sci USA* 1997; 94: 5450-5455.
22. Sabbah HN, Stein PD, Kono T, et al. A canine model of chronic heart failure produced by multiple sequential coronary microembolizations. *Am J Physiol Heart Circ Physiol* 1991; 29: H1379-H1384.
23. Kumar S, Seqqat R, Chigurupati S, et al. Inhibition of nuclear factor kB regresses cardiac hypertrophy by modulating the expression of extracellular matrix and adhesion molecules. *Free Radical Biology & Medicine* 2011; 50: 206-215
24. Gupta S, Young D, Maitra RK, et al. Prevention of cardiac hypertrophy and heart failure by silencing of NF-kappaB. *J. Mol. Biol* 2008; 375: 637-649;
25. Li H, Gu H, Sun B. Protective effects of pyrrolidine dithiocarbamate on myocardium apoptosis induced by adriamycin in rats. *Int J Cardiol* 2007; 114(2):159-65.
26. Zeng M, Yan H, Chen Y, et al. Suppression of NF- κ B reduces myocardial no-reflow. *PLoS One* 2012; 7: e47306-47316.

27. Olivetti G, Quaini F, Sala R, et al. Acute myocardial infarction in humans is associated with activation of programmed myocyte cell death in the surviving portion of the heart. *J Mol Cell Cardiol* 1994; 28: 2005–2016.
28. Brian R. Weil, Rebeccah F. Young, Xiaomeng Shen, et al. Brief Myocardial Ischemia Produces Cardiac Troponin I Release and Focal Myocyte Apoptosis in the Absence of Pathological Infarction in Swine. *JACC Basic Transl Sci* 2017; 2: 105–114.
29. Frustaci A, Chimenti C, Setoguchi M, et al. Cell death in acromegalic cardiomyopathy. *Circulation* 1999; 99: 1426–1434.
30. Condorelli G, Morisco C, Stassi G, et al. Increased cardiomyocyte apoptosis and changes in proapoptotic antiapoptotic genes bax and bcl-2 during during left ventricular adaptation to chronic pressure overload in the rat. *Circulation* 1999; 99: 3071–3078
31. Charis Putinski, Mohammad Abdul-Ghani, Rebecca Stiles, et al. Intrinsic-mediated caspase activation is essential for cardiomyocyte hypertrophy. *Proc Natl Acad Sci USA* 2013; 110: E4079–E4087.
32. Gino A. Kurian, Rashmi Rajagopal, Srinivasan Vedantham, et al. The role of oxidative stress in myocardial ischemia and reperfusion injury and remodeling: revisited. *Oxid Med Cell Longev*. 2016; 2016: 1656450.
33. David M. Ansley and Baohua Wang. Oxidative stress and myocardial injury in the diabetic heart. *J Pathol* 2013; 229: 232–241.

Group	SML(%)
Sham	0.66 ± 0.35
HFU	21.25 ± 3.54
	P<0.001##
HFP	15.38 ± 2.50
	P=0.001**

#P<0.05, ##P<0.01 vs Sham; *P<0.05, **P<0.01 vs HFU.

Group	apoptosis index (%)			
	1d	3d	7d	14d
Sham	1.42±0.74	1.50±0.63	1.25±0.52	1.25±0.61
HFU	13.33±2.16	19.67±2.58	11.50±2.74	7.17±1.47
	P<0.001##	P<0.001##	P<0.001##	P<0.001##
HFP	5.00±1.41	10.50±1.87	4.95±1.31	2.83±0.75
	P<0.001**	P<0.001**	P=0.003**	P<0.001**

#P<0.05, ##P<0.01 vs Sham; *P<0.05, **P<0.01 vs HFU.

Table 3. Effects of PDTC on cardiac function assessed hemodynamically and echocardiographically						
Groups	HR (beats/min)	LVSP (mmHg)	LV dp/dtmax (mmHg.s⁻¹)	LV -dp/dtmax (mmHg.s⁻¹)	LVE (%)	LVEDP (mmHg)
Sham						
1d	338 ± 30	128 ± 8	5267 ± 1049	4975 ± 695	90 ± 3	4 ± 1
3d	334 ± 15	129 ± 13	5236 ± 852	4882 ± 455	88 ± 3	3 ± 1
7d	344 ± 23	130 ± 10	5440 ± 975	4878 ± 677	89 ± 4	3 ± 1
14d	335 ± 27	135 ± 10	5707 ± 544	4974 ± 767	90 ± 4	3 ± 1
HFU						
1d	449 ± 12	102 ± 89	2826 ± 852	2682 ± 247##	60 ± 4	20 ± 5
	P<0.001##	P<0.001##	P<0.001##	P<0.001##	P<0.001##	P<0.001##
3d	426 ± 21	104 ± 15	2956 ± 464	2676 ± 385##	65 ± 5	20 ± 5
	P<0.001##	P=0.002##	P<0.001##	P<0.001##	P<0.001##	P<0.001##
7d	459 ± 18	101 ± 10	3033 ± 358	2634 ± 592##	61 ± 4	18 ± 4
	P<0.001##	P<0.001##	P<0.001##	P<0.001##	P<0.001##	P<0.001##
14d	442 ± 27	100 ± 10	2918 ± 276	2481 ± 365##	61 ± 6	18 ± 2
	P<0.001##	P<0.001##	P<0.001##	P<0.001##	P<0.001##	P<0.001##
HFP						
1d	409 ± 30	119 ± 11	3932 ± 428	3642 ± 492	75 ± 5	14 ± 2
	P=0.001**	P=0.002**	P=0.006**	P=0.002**	P=0.001**	P=0.002**
3d	382 ± 19	120 ± 10	4380 ± 334	4016 ± 265	78 ± 2	14 ± 3
	P<0.001**	P=0.031**	P=0.001**	P=0.001**	P<0.001**	P=0.001**
7d	365 ± 26	123 ± 14*	4419 ± 53	4252 ± 339	80 ± 3	13 ± 2
	P<0.001**	P=0.002**	P=0.001**	P<0.001**	P<0.001**	P=0.001**
14d	362 ± 31	126 ± 13	4828 ± 289	4398 ± 269	80 ± 4	13 ± 1
	P<0.001**	P<0.001**	P<0.001**	P<0.001**	P<0.001**	P<0.001**

Data are mean ± SD, #P<0.05, ##P<0.01 vs Sham; *P<0.05, **P<0.01 vs HFU. HR, heart rate; LVSP, left ventricular systolic pressure; LV +dp/dt max, maximum rate of left ventricular pressure rise; LV -dp/dt max, maximum rate of left ventricular pressure relax; LVEF, left ventricular ejection fraction.

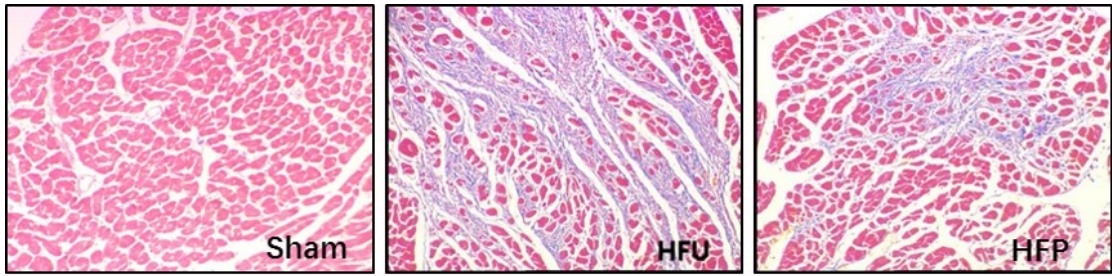


Fig1. Effects of PDTC on myocardial fibrosis by Masson's trichrome staining on day 14 ($\times 200$)

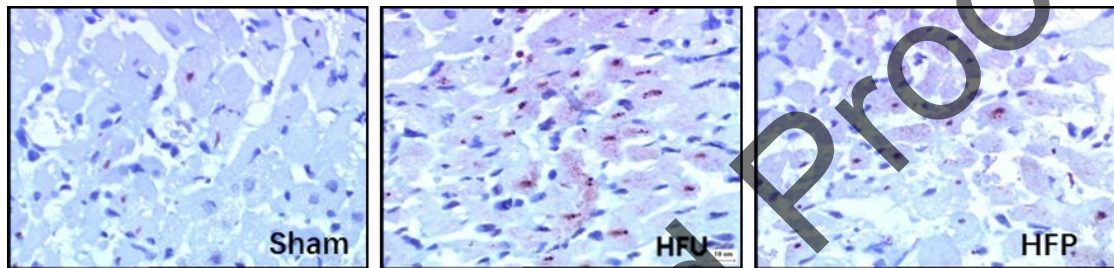


Fig 2. The changes of myocardial apoptosis by TUNEL on day 3 ($\times 400$)

Uncorrected Proof